Walking Selectively Modulates Behaviorally Relevant Auditory Responses According to Stride Cycle Phase

Ishrat mehmood[1 ,2 ,3 ,4, 5, 6, #], Haoxuan Xu[4, 5, 6, #], Peirun Song[1, 4], Yuying Zhai[1, 3], Cheng Chang[1], Xuehui Bao[4], Hangting Ye[4], Sirou Guo[1],Yanyan Wang[3], Lingling Zhang[3], Pei Chen[3], Wanshun Wen[7], Xuan Zhao[3], Gang Chen[2] and Xiongjie Yu[1, 2, 3, 4 ,5, 6]*

[1]Department of Anesthesia, Women's Hospital, Zhejiang University School of Medicine, Hangzhou, China

[2]Oujiang Laboratory (Zhejiang Lab for Regenerative Medicine, Vision and Brain Health), Wenzhou, Zhejiang, China;

[3]Department of Anesthesiology, Shanghai Tenth People's Hospital, Tongji University School of Medicine, Shanghai, China

[4]Zhejiang Provincial Key Laboratory of Precision Diagnosis and Therapy for Major Gynecological Diseases, Women's Hospital, Zhejiang University School of Medicine, Hangzhou, China

[5]College of Biomedical Engineering and Instrument Science, Zhejiang University, Hangzhou, China

[6]Key Laboratory for Biomedical Engineering of Ministry of Education, Zhejiang University, Hangzhou, China

[7]Center for Rehabilitation Medicine, Rehabilitation and Sports Medicine Research Institute of Zhejiang Province, Department of Rehabilitation Medicine, Zhejiang Provincial People's Hospital, Affiliated People's Hospital, Hangzhou Medical College, Hangzhou, Zhejiang, China

[#]These authors contributed equally

[*] Corresponding author and Lead contact: yuxiongj@ gmail.com (X.Y.)

Running Title: Walking Differently Modulates Auditory Responses

Key Words: Locomotion; EEG; Auditory temporal integration; Change detection;

Author contributions: Conceptualization, X.Y.; Methodology, X.Y.; Investigation and Data Curation, I.M., H.X., P.S., and Y.Z.; Writing – Original Draft, X.Y., I.M. and H.X.; Writing – Review & Editing, I.M., H.X., P.S., C.C., Y.W., S.G., L.Z., P.C., X.Y., W.W., X.Z., G.C. and X.Y.; Funding Acquisition, X.Y., X.Z. and Y.Z.; Resources, X.Y.; Software, I.M., H.X., P.S., Y.Z., X.B. and H.Y.; Validation and Visualization, I.M. and H.X.; Supervision, X.Y.

Declaration of interests: The authors declare no competing interests.

Acknowledgements. We are grateful to Profs. Xiaoming Zhou, Nai Ding and Xi Chen for their invaluable comments on the early version of the manuscript, as well as to Xiaokai Kou for the help with the experiments. This work was supported by STI2030-Major Projects (2022ZD0204600 and 2022ZD0204800) (to X.Y.); National Natural Science Foundation of China 32171044 (to X.Y.), and 32100827 (to Y.Z.); Key Support Discipline Construction Project of Shanghai Municipal Health Commission 2023ZDFC0203 (to X.Z.).

Abstract

Human perception operates in dynamic environments, requiring sensory processing to continuously adapt to ongoing motor activity. Here, we investigated how natural walking modulates auditory change detection by recording EEG while participants performed a transitional click train task during sitting and walking. Behaviorally, walking significantly elevated auditory change detection thresholds, reflecting reduced perceptual sensitivity. Electrophysiologically, three distinct auditory responses onset, change, and offset were evoked; both the onset and change responses were attenuated during walking, with the most pronounced effect observed for the cognitively demanding change response. Notably, this modulation was further amplified for the change response during active engagement compared to passive listening, implicating attentional resource allocation. Strikingly, both behavioral performance and change-related neural responses fluctuated rhythmically with the gait cycle, while onset and offset responses remained comparatively stable. Together, these findings reveal a stride-phase-dependent gating mechanism that selectively modulates perceptually relevant auditory signals, illustrating how the brain rhythmically reallocates sensory resources to optimize perception during locomotion.

Introduction

Human perception is an inherently active process, continuously shaped by interactions with a dynamic sensory environment (Li, Muschter et al. 2021). Sensory systems, including vision, touch, and hearing, integrate incoming stimuli to construct a cohesive perception of the external environment (Lickliter 2011). Among the sensory modalities, audition plays a critical role in detecting and interpreting temporally complex information such as speech, music, and environmental sounds (Rauschecker 1998). Importantly, auditory perception does not operate in isolation but is deeply embedded within the context of ongoing bodily movements, including speech articulation and hand movements related to writing or finger tracing (Donato, Contillo et al. 2024, Zheng, Zhang et al. 2025). Natural behaviors, such as walking, running, or exploring the environment, not only alter the spatial orientation of sensory organs but also influence central sensory processing (Parker, Brown et al. 2020). While psychological evidence has shown that walking modulates visual perception—producing rhythmic fluctuations in detection performance aligned with the gait cycle (Davidson, Verstraten et al. 2024)—it remains unclear whether similar motor-related modulation occurs in the auditory domain, and what neural correlates underlie such modulation during walking. Accordingly, it is essential to examine this phenomenon not only at the psychological level but also through electrophysiological investigation.

A key process in auditory perception is temporal integration—the brain's ability

to combine discrete acoustic events into unified perceptual streams. This mechanism underlies our experience of temporal pitch in rapidly presented click trains, where inter-click intervals (ICIs) shorter than ~33 ms are no longer perceived as discrete pulses but as a single, fused tone. Transitional click trains, comprising two sequential click trains with subtly differing ICIs, are well suited for probing this integration process (Song, Xu et al. 2025, Xu, Huang et al. 2025). At the transition between trains, listeners perceive a pitch shift, which elicits a robust neural signature known as the change response, indexing perceptual updating and temporal integration (Kraus, Skoe et al. 2009). Complementing this, the offset response, traditionally linked to sound termination, has recently been shown to reflect sensitivity to both stimulus duration and ICI, suggesting a broader role in encoding temporally structured input (Song, Xu et al. 2024). Alongside these, the onset response—elicited at the start of auditory input—serves as a canonical marker of early, bottom-up auditory detection (Nabé, Schwartz et al. 2021). Together, these three electrophysiological responses—onset, change, and offset—provide a multidimensional framework for dissecting how natural locomotion shapes auditory processing under different behavioral states. Importantly, because these responses differ in their cognitive demands and functional significance, they allow us to distinguish between general effects of walking on auditory neural activity and those that arise specifically when active perceptual engagement is required, highlighting the selective modulation of behaviorally relevant auditory responses. The onset and offset responses reflect more automatic, bottom-up processing, whereas the change response reflects higher-level perceptual integration

and updating. By contrasting their modulation during walking, we can discern whether locomotion imposes a uniform effect on auditory encoding or preferentially targets cognitively demanding, behaviorally salient processes.

To address these questions, we employed electroencephalography (EEG) to record auditory neural responses while participants performed a change detection task with transitional click trains under both sitting and natural walking conditions. By systematically examining how onset, change, and offset responses are modulated across different phases of the stride cycle, we sought to determine whether locomotion exerts a general effect on auditory processing or selectively modulates behaviorally relevant neural signals. This approach enables us to uncover how natural locomotion rhythmically structures auditory perception during goal-directed behavior and elucidate the neural mechanisms underlying motor-sensory interactions in dynamic environments.

Results

Walking Elevates the Threshold for Auditory Change Detection

We assessed auditory change detection using transitional click trains under two conditions: natural walking and sitting (Fig. 1a). Each stimulus comprised two concatenated 1-s regular click trains with differing inter-click intervals (ICIs): the first (Train 1) fixed at 4 ms, and the second (Train 2) at varying ICIs, such as 4.06 ms in the Reg4–4.06 configuration (Fig. 1b, top). To probe sensitivity systematically, Train 2 ICIs spanned five contrast levels (0%, 0.25%, 0.5%, 0.75%, and 1.5%) relative to

the 4-ms baseline. Trials consisted of the 2-s stimulus followed by a 2-s response window, during which participants reported perceived changes via button press (Fig. 1b). The task alternated between walking and sitting blocks, with 50 trials per condition.

Behavioral data showed markedly reduced change detection during walking compared to sitting, as evidenced by rightward-shifted psychometric functions ($n = 47$; Fig. 1c). Most participants displayed higher thresholds in walking ($t(46) = 16.36$, $p < 0.001$, paired t-test; Fig. 1d), indicating that locomotion impairs auditory temporal discrimination and elevates the perceptual threshold for subtle acoustic changes.

Locomotion-Induced Modulation of Onset, Change, and Offset Responses

Building on the behavioral findings, we next analyzed corresponding neural activity via EEG. Transitional click trains consistently evoked three distinct auditory responses: onset, change, and offset (Fig. 2a). We compared these across sitting and walking conditions. At a representative electrode (P4), onset responses were broadly similar but showed modestly higher amplitude during sitting in the 108–208 ms post-onset window ($p < 0.05$, permutation test). By contrast, the change response was markedly attenuated during walking, especially 173–280 ms post-transition ($p < 0.05$, permutation test), whereas the offset response exhibited no significant difference. These patterns suggest that locomotion selectively suppresses change-related neural activity while sparing termination encoding.

At the group level ($n = 47$), we quantified response magnitude (RM) differences between conditions (Fig. 2b). Onset data were pooled across all stimuli, given the

invariant initial Reg_4 segment. Significant attenuation occurred for onset ($t(46) = 3.52$, $p < 0.001$, $d = 0.51$, paired t-test) and change responses at higher contrasts ($Reg_{4\text{-}4.02}$, $Reg_{4\text{-}4.03}$, and $Reg_{4\text{-}4.06}$; all $p < 0.001$), but not for offset, underscoring response-specific modulation by walking.

Topographic maps of RM differences (sit – walk) revealed spatial patterns (Fig. 2c). Onset modulation involved 27 significant electrodes ($p < 0.05$, t-test, FDR-corrected), mainly bilateral parietal. Change modulation was contrast-dependent: minimal at low contrasts ($Reg_{4–4}$, $Reg_{4–4.01}$), peaking at $Reg_{4–4.02}$ (54 electrodes significant), and tapering to 32 electrodes at $Reg_{4–4.06}$, aligning with perceptual demands near threshold. Offset showed negligible effects, with no significant electrodes.

To further characterize these effects, we computed ΔRM (sit – walk) as a function of ICI contrast (Fig. 2d). For the change response, the amplitude difference increased from $Reg_{4–4}$ to $Reg_{4–4.02}$, then slightly decreased at $Reg_{4–4.06}$, yielding a non-monotonic profile ($F(4, 230) = 16.09$, $p < 0.001$, $\eta^2 = 0.22$, one-way ANOVA; Fig. 2d, middle panel). Notably, the RM difference for the change response at $Reg_{4–4.02}$ exceeded that of the onset response, suggesting more prominent modulation for the change response. In contrast, the offset response showed no significant variation across contrast levels ($F(4, 230) = 0.66$, $p = 0.62$, $\eta^2 = 0.01$, BF10 = 0.01, ANOVA; Fig. 2d, right panel), reinforcing the interpretation that walking selectively influences perceptual updating mechanisms reflected in the change response, rather than more automatic auditory processes such as offset encoding.

Active Versus Passive Listening: Differential Neural Effects of Walking

Given that participants were actively engaged in detecting auditory changes, we hypothesized that the observed modulation of the change response might depend on task engagement. To test this, we conducted a passive listening control experiment in which participants alternated between sitting and walking while listening to the same stimuli but performed no behavioral task (Fig. 1).

In the same representative channel (P4), onset responses remained largely similar between walking and sitting. The change response, however, still showed attenuation during walking within the 174–244 ms window following the click train transition ($p < 0.05$, permutation test; Fig. 3a). The offset response again showed no significant difference. These results suggest that walking suppresses change-related neural responses even in the absence of an explicit behavioral task.

At the population level, RM comparisons mirrored. Significant differences were found for the onset response ($n = 21$, $Z = 2.69$, $p < 0.01$, $r = 0.59$, Wilcoxon signed rank test; Fig. 3b), and for the change response at $Reg_{4–4.02}$, $Reg_{4–4.03}$, and $Reg_{4–4.06}$ ($p < 0.01$, Wilcoxon signed rank test; Fig. 3b). The offset response again showed a significant RM difference only at $Reg_{4–4.01}$ ($Z = 2.83$, $p < 0.01$, $r = 0.62$, Wilcoxon signed rank test; Fig. 3b), confirming its overall insensitivity to task or motor state.

We next assessed the spatial distribution of modulation during passive listening using the same topographic analysis of RM difference (Fig. 3c). For the onset response, 21 electrodes showed significant differences ($p < 0.05$, Wilcoxon signed rank test, FDR corrected), mainly over parietal and occipital regions. In contrast, the

change response exhibited a different pattern: no significant electrodes were observed at low contrast levels ($Reg_{4–4}$ to $Reg_{4–4.02}$), whereas 23 electrodes reached significance at $Reg_{4–4.03}$, and 5 at $Reg_{4–4.06}$. These findings suggest that walking-related modulation of the change response persists without task engagement but is weaker and requires larger stimulus contrasts. The offset response again showed minimal modulation, with no significant electrodes across contrast levels.

To determine whether task engagement amplifies the modulatory effect of walking, we directly compared RM differences between active and passive conditions. For the onset and offset responses, no significant differences were observed between the two conditions, indicating that walking modulates these responses similarly regardless of behavioral engagement. In contrast, the change response showed significantly stronger modulation in the active condition at $Reg_{4–4.02}$ ($Z = 2.50$, $p < 0.05$, $r = 0.30$, Mann-Whitney U test; Fig. 3d), suggesting that perceptual engagement selectively amplifies the effect of walking, particularly near the detection threshold. Collectively, walking modulates auditory responses in a type- and contrast-specific manner: offset is stable, while change is locomotion-sensitive and task-augmented, highlighting dynamic interplay among motor state, demand, and change encoding.

Response Oscillates Within the Stride Cycle

After characterizing the effects of walking on the three types of auditory responses during the change detection task, we next investigated whether both behavioral and neural responses were modulated by the phase of the stride cycle. To ensure comprehensive sampling across all gait phases, we focused on three stimulus

conditions—$Reg_{4–4}$, $Reg_{4–4.02}$, and $Reg_{4–4.06}$—randomly presenting approximately 100, 200, and 300 trials per participant, respectively, during walking. Analyses centered primarily on the $Reg_{4–4.06}$ condition, which offered the highest trial count and the most robust change responses.

Walking speed was monitored and confirmed to be stable at approximately 1 Hz, as determined by Fourier analysis. For stride-phase alignment, each stride was resampled to span 1–100% of the gait cycle in one example subject (Fig. 4a), allowing for both within- and across-participant averaging. Auditory stimuli were presented at random time points, and neural responses—onset, change, and offset—were assigned to the corresponding stride positions. This approach enabled the pooling of hundreds of trials into a single, densely sampled gait cycle, subsequently divided into fine-grained time bins for detailed temporal analysis (Fig. 4b). Importantly, the dataset exhibited a uniform distribution of response timings across stride phases for all three response types, confirming consistent sampling and ruling out phase-dependent presentation bias. This uniformity validates subsequent analyses of rhythmic modulation.

We first analyzed behavioral performance at $Reg_{4–4.06}$. Subjects with perfect (100%) hit rates at $Reg_{4–4.06}$ were excluded, as their lack of variability precluded assessment of rhythmic modulation. Hit rates were aligned to the timing of sound onset, which was randomized with respect to stride phase and then assigned to a position within the gait cycle (1–100%). Figure 4c presents the group-averaged hit rates (n = 21), binned into 10 equal, non-overlapping intervals. Green solid curves

represent best-fitting first-order Fourier models. When aligned to onset, no significant oscillatory pattern was observed in detection performance ($p = 0.21$, permutation test, left panel, Fig. 4c). In contrast, clear oscillatory patterns in hit rate emerged when responses were aligned to the change point ($p < 0.05$, permutation test, middle panel, Fig. 4c), whereas no oscillation was observed for alignment with the offset ($p = 0.14$, permutation test, right panel, Fig. 4c). To quantify these effects, we computed the goodness-of-fit (R^2) for all Fourier frequencies from 0.2 to 4 cycles per stride (cps) in 0.1 cps increments. For hit rate, the best-fitting oscillation occurred at 2.65 cps ($R^2 = 0.74$) when aligned to the change point. Group-level fits exceeded the 95th percentile of the permutation-based null distribution ($n = 1000$) over the range of 2.4–3 cps (Fig. 4d), indicating that the oscillation was statistically significant and not attributable to chance. These findings demonstrate that behavioral sensitivity to auditory changes fluctuates rhythmically with the stride cycle when aligned with the change point, but not with onset or offset.

A similar pattern was observed for reaction times. Oscillatory modulation was present only when trials were aligned with the change point, not with onset or offset (Fig. 4e). The best-fitting oscillation for reaction time occurred at 2.36 cps for the change point and was significant within the range of 2.1–2.5 cps (Fig. 4f), further supporting the conclusion that behavioral performance is rhythmically modulated in phase with gait only at the change point.

We then examined the EEG results. All subjects were included in this analysis, as EEG variability is present irrespective of behavioral variability. Responses were

binned into 10 equal, non-overlapping stride-phase intervals relative to the timing of the onset, change, and offset components. The corresponding average EEG amplitudes are shown in Fig. 5a, and their root-mean-square (RMS) values across phases are plotted in Fig. 5b. Solid colored curves indicate best-fitting first-order Fourier models. No significant oscillation was observed when responses were aligned to onset or offset (left and right panels, Fig. 5b). In contrast, when aligned to the change point, neural responses exhibited a robust oscillatory pattern ($p = 0.02$, permutation test, middle panel, Fig. 5b). The best-fitting frequency was 1.58 cps ($R^2 = 0.71$), and group-level fits exceeded the 95th percentile of the null distribution within the 1.4–1.8 cps range (Fig. 5c), confirming statistical significance.

A topographic analysis of R^2 values across all 64 electrodes revealed widespread and significant modulation for the change response, with substantially higher values than those observed for onset or offset ($p < 0.05$ for both comparisons, FDR corrected; Fig. 5d). These results indicate that the neural encoding of auditory change is rhythmically modulated in synchrony with the stride cycle, in contrast to the relatively stable onset and offset responses.

Discussion

In this study, we systematically investigated how natural walking modulates auditory change detection performance and its underlying neural correlates. Using a transitional click train paradigm, we found that walking significantly increased the perceptual threshold for detecting auditory changes, as shown by markedly reduced behavioral sensitivity during walking compared to sitting (Fig.1c, d). This

demonstrates a substantial impact of locomotion on the perception of subtle temporal changes in sound. At the neural level, EEG recordings revealed that walking differentially affected distinct types of auditory-evoked responses. Both the onset and change responses were attenuated during walking, but this effect was most pronounced for the change response—a neural marker closely associated with temporal integration (Fig. 2a–c). In contrast, the offset response remained relatively stable across conditions. Importantly, the attenuation of the change response was amplified during active behavioral engagement and was less pronounced under passive listening, indicating a critical role for attention and task demands in this modulation (Fig. 3a–c). Finally, by aligning neural and behavioral data to the phase of the gait cycle, we observed robust oscillatory modulation of both behavioral performance (Fig. 4) and the change response (Fig. 5) across the stride. In contrast, onset and offset responses did not exhibit significant phase-dependent variation. These findings suggest that sensitivity to auditory change is rhythmically gated in synchrony with locomotor dynamics, revealing a selective and dynamic interplay between movement and auditory processing.

Preferential Modulation of the Behavior Relevant Response

A central finding of our study is the selective attenuation of both the onset response and, most notably, the change response during walking. Unlike the more automatic onset and offset responses, the change response was significantly diminished, especially under near-threshold conditions (Fig. 2). We propose that this walking-induced effect arises from the distinct cognitive demands associated with

each neural response. The onset response reflects the initial, largely bottom-up detection of an acoustic stimulus (Nabé, Schwartz et al. 2021), while the offset response marks the termination of an integrated auditory object (Song, Xu et al. 2024). In contrast, detecting subtle shifts in ICI within a transitional train requires a more demanding, top-down process of continuous temporal integration and comparison (Asilador and Llano 2020), a process that is particularly taxing near the perceptual threshold (Fig. 2b). This higher-order integration likely depends on neural networks that actively maintain and update internal representations of a sound's temporal structure. Previous research has shown that higher-order sensory processing can be affected by concurrent tasks, such as locomotion, with movement -related signals influencing sensory processing (Parker, Brown et al. 2020). Indeed, multitasking that involves simultaneous cognitive and motor demands has been demonstrated to impair sensory processing efficiency (Davidson, Verstraten et al. 2024). These findings are consistent with studies reporting that temporal integration in sensory processing is particularly vulnerable to disruption by concurrent motor activity, underscoring the susceptibility of higher-order auditory functions to motor demands (Tallal, Miller et al. 1993, Zagha, Casale et al. 2013, Dionne-Dostie, Paquette et al. 2015), further emphasizing the brain's prioritization of behaviorally relevant signals during resource competition.

Walking itself is not a purely automatic activity; it requires considerable cognitive resources for balance, navigation, and the integration of multisensory feedback (visual, vestibular, proprioceptive) (Parker, Brown et al. 2020). The increased cognitive-motor

load during walking likely creates competition for limited neural resources—a phenomenon supported by research indicating that multitasking reduces available cognitive resources, particularly in complex environments (Salvucci and Taatgen 2008, Tomassini, Spinelli et al. 2015). As a result, resource-intensive processes, such as detecting temporal pitch changes, are more susceptible to interference than less demanding processes underlying onset and offset responses. This dynamic interplay suggests that the brain prioritizes certain cognitive tasks when motor activity requires substantial attentional resources (Zheng, Zhang et al. 2025), thereby optimizing overall efficiency in dynamic contexts.

Our results further demonstrate that active behavioral engagement amplifies the modulatory effect of walking, particularly under near-threshold conditions (Fig. 3), providing strong evidence for an attentional mechanism. Under passive listening conditions, where no explicit temporal comparison is required, the modulation of the change response by walking is less pronounced than during active engagement. In contrast, the modulation of the onset and offset responses by walking remains relatively unchanged across active and passive conditions. This pattern suggests that the observed attenuation reflects not only low-level sensory gating by movement but also a higher-order consequence of dual-task interference (Liebherr, Corcoran et al. 2021, McPhee, Cheung et al. 2022, Riedel, Herzog et al. 2024), wherein the brain must allocate limited attentional resources between the competing demands of walking and active auditory processing. Collectively, these observations establish a logical progression from general locomotor suppression to task-amplified, selective

gating, underscoring the adaptive nature of sensorimotor interactions.

Rhythmic Modulation of Auditory Perception by the Stride Cycle

Our findings reveal that the impact of walking on auditory perception is not simply a general effect, but is characterized by rhythmic modulation synchronized with the stride cycle (Fig. 4). This demonstrates that the allocation of neural resources for auditory change detection fluctuates dynamically with each step, rather than remaining constant throughout locomotion. Notably, our behavioral results (Fig. 4) parallel recent work in the visual domain, where detection performance oscillates in synchrony with gait, exhibiting distinct phases of optimal and suboptimal sensitivity within the stride cycle (Tomassini, Spinelli et al. 2015, Davidson, Verstraten et al. 2024). Comparable patterns have also been reported in the somatosensory system, where tactile perception fluctuates rhythmically in concert with balance control, underscoring the complex interplay between sensory processing and motor states (Wachsmann, Fiehler et al. 2025). Building on these cross-modal parallels, recent studies further indicate that such oscillatory patterns in sensory systems are not only temporally linked to motor activity but also influence the timing and precision of sensory processing, including in audition (Morillon, Schroeder et al. 2014, Morillon and Baillet 2017, Proksch, Comstock et al. 2020, Gong, Song et al. 2024, Auksztulewicz, Ödül et al. 2025, Du, Xu et al. 2025) , thereby establishing a foundation for domain-general entrainment mechanisms.

Crucially, our study provides the first electrophysiological evidence that gait-phase-dependent oscillations extend to auditory change detection (Fig. 5),

supporting the notion of a domain-general mechanism for motor-sensory entrainment during active behavior. This observation is consistent with theoretical models that propose multisensory integration across domains—including auditory and visual perception—is rhythmically aligned with bodily movement, illustrating how diverse sensory modalities are entrained to the motor system (Starke, Ball et al. 2020, Senkowski and Engel 2024, Di Stefano and Spence 2025). Complementing these models, additional research suggests that such rhythmic entrainment of sensory processing reflects an adaptive mechanism that enhances sensory efficiency by aligning cognitive resources to the most favorable phase of the motor cycle (Zalta, Petkoski et al. 2020, Pranjić, Braun Janzen et al. 2024, Noboa, Kertész et al. 2025), linking behavioral observations to underlying neural dynamics.

These oscillations may likely reflect "windows of opportunity" within the motor cycle. Certain phases of the stride, such as the double support phase (heel-strike), are more stable and may require less active control and sensory feedback compared to the more dynamic swing phase. This observation is consistent with biomechanical evidence showing reduced cortical engagement during stable gait phases (Stuart, Vitorio et al. 2018, Delval, Bayot et al. 2020, Rubega, Di Marco et al. 2021). The reduction in cortical activity during stable phases aligns with the previous findings that reported reduced sensorimotor integration during low-movement phases in their tactile perception studies, thereby supporting the notion that certain stride phases allow the brain to allocate resources to other sensory modalities, including auditory processing (Hentschke, Haiss et al. 2006). Consequently, more neural resources may

be momentarily freed during these stable phases for allocation to other cognitive tasks, such as auditory change detection. The fact that only the most cognitively demanding neural signature—the change response—was coupled to this rhythm further reinforces the resource competition framework. Our results suggest that the brain rhythmically prioritizes neural resources, with the auditory process most susceptible to interference becoming entrained to the body's movements. This dynamic allocation strategy likely reflects an active optimization of sensory integration and motor control, enabling the brain to maintain perceptual efficiency during complex, real-world behaviors.

Materials and Methods

Experimental Procedure and Participants

This study encompassed three experiments, conducted in compliance with the Declaration of Helsinki (2013) and approved by the Institutional Review Board (IRB-20230131-R). Informed consent was obtained from all participants. Experiment 1 (behavioral and neural) involved 47 healthy adults (28 males, 19 females; mean age 22.98 ± 2.72 years). Experiment 2 (passive listening) included 21 healthy adults (12 males, 9 females; mean age 23.90 ± 3.88 years). Experiment 3 (behavioral and neural during stride cycle) comprised 57 healthy adults (36 males, 21 females; mean age 23.12 ± 2.78 years), with 21 healthy adults (11 males, 10 females; mean age 23.38 ± 2.17 years) were selected for behavioral analysis based on $Reg_{4\text{-}4.06}$ hit rates below 100% under each stride cycle bin. Participants maintained a stationary head position

while listening to stimuli in sitting and walking conditions, responding via wireless button press.

Experiment 1: A change detection task in alternating sitting and walking blocks to probe perceptual and neural correlates of auditory processing. In sitting, participants sat with a wireless key and chest-mounted speaker; in walking, they moved at normal pace (~1 m/s, ~1 Hz stride frequency, monitored via inertial sensors) in a soundproof room with the same setup (Fig. 1a). They reported changes by pressing keys (right for change, left for none) within 2 s post-stimulus. Five transitional click trains ($Reg_{4\text{-}4}$, $Reg_{4\text{-}4.01}$, $Reg_{4\text{-}4.02}$, $Reg_{4\text{-}4.03}$, $Reg_{4\text{-}4.06}$) were randomized (~40 trials each), followed by an 800-ms delay and 100-ms 1kHz cue; responses valid within 2 s of cue (Fig. 1b). Behavioral (Fig.1c, d) and neural (Fig.2a-d) analyses covered all trains, assessing sensitivity to ICI differences across conditions.

Experiment 2: Passive listening in sitting and walking to evaluate baseline neural responses without cognitive load, using identical stimuli (~40 trials each). Setups mirrored Experiment 1. Analyses (Fig.3a-c) examined neural sensitivity to ICI variations.

Experiment 3: Change detection during walking to assess stride-phase effects on perceptual and neural auditory processing. The setup matched Experiment 1's walking condition (Fig.1a, b), in a single block. Three trains ($Reg_{4\text{-}4}$, $Reg_{4\text{-}4.02}$, $Reg_{4\text{-}4.06}$) were randomized (~100, 200, 300 trials). Behavioral (Fig.4c-f) and neural (Fig.5a-d) analyses evaluated phase-dependent sensitivity.

Auditory Stimuli

All experiments were conducted in a soundproof room. Each click consisted of a 0.2-ms monopolar pulse (Fig.1b). Regular click trains featured fixed inter-click intervals (ICIs) without randomization. Transitional click trains were formed by concatenating two regular trains with differing fixed ICIs—for instance, $Reg_{4\text{-}4.06}$ combined a 4-ms ICI train followed seamlessly by a 4.06-ms ICI train. Contrasts were defined as 0%, 0.25%, 0.5%, 0.75%, and 1.5% relative to the 4-ms baseline ICI. Stimuli were delivered through a Golden Field M23 speaker, powered by a Creative AE-7 Sound Blaster at a sampling rate of 384 kHz, and controlled via Psychtoolbox 3 in MATLAB. Sound intensity was calibrated to a constant 60 dB SPL using a ¼-inch Brüel & Kjær 4954 condenser microphone and PHOTON/RT analyzer.

Data Acquisition

EEG data for all three experiments were acquired using a 64-channel NeuSenW system (Neuracle, China), with 59 electrodes active in practice. Ground electrodes were positioned between Fpz and Fz in the frontal region. The reference electrode was placed between Cz and Pz, replacing CPz in the wireless EEG cap. Concurrent with high-density EEG signals, embedded inertial sensors captured movement data at 100 Hz, facilitating synchronized monitoring of brain activity and dynamics. EEG was sampled at 1 kHz, with electrode placement adhering to the international 10-20 system.

Data Analysis

Preprocessing

Data analyses were performed using MATLAB R2021b (The MathWorks, Inc., Natick,

MA, USA) and the FieldTrip toolbox (Oostenveld, Fries et al. 2011). Monopolar referencing was applied using the default reference electrode positioned between Cz and Pz. Multichannel EEG data underwent sequential preprocessing: initial bandpass filtering (0.5–40 Hz), followed by epoch extraction from -1 to 3 s relative to trial onset. Independent component analysis (ICA) removed electrooculogram (EOG) artifacts. Baseline correction subtracted the mean activity from -200 to 0 ms pre-stimulus onset per trial. Motion artifacts were evaluated via a relative threshold, flagging samples outside mean ± 3 SD as "bad." Trials exceeding 20% bad samples were discarded as "bad trials," and channels with >10% bad trials were labeled "bad channels." Bad channels were excluded first (based on all-channel data), followed by bad trials from remaining channels. Event-related potentials (ERPs) were computed by averaging epochs per experimental condition, channel, and subject. Prior to group-level analysis, ERPs were normalized by dividing each channel's data by its standard deviation per subject to minimize inter-channel variability.

Permutation test

Permutation tests for time-point and channel-wise comparisons of event-related potential (ERP) data between conditions (sitting vs. walking) employed a two-tailed cluster-based approach via the 'ft_timelockstatistics' function in the FieldTrip toolbox for MATLAB. A two-tailed independent-samples t-test was conducted at each time point and channel to compute t-values, contrasting Dataset A (ERP data for $Reg_{4\text{-}4.06}$ in the sitting condition) and Dataset B (ERP data for $Reg_{4\text{-}4.06}$ in the walking condition) across 47 participants. A cluster-defining threshold of $p < 0.05$ identified significant

time points, which were grouped into clusters based on temporal adjacency (consecutive significant time points) and spatial proximity (neighbouring electrodes). Condition labels for Datasets A and B were randomly permuted, generating a new t-value matrix per iteration; clusters were reformed using the same $p < 0.05$ threshold. The largest cluster-level statistic (e.g., sum of t-values) from each of 1000 permutations formed the null distribution. Observed clusters were deemed significant if their statistic exceeded the 95th percentile of this distribution ($p < 0.05$). Tests spanned the time window of -500 to 2500 ms relative to the transitional click train onset. For instance, Dataset A comprised ERP data for $Reg_{4\text{-}4.06}$ in sitting from 47 participants, while Dataset B comprised corresponding data in walking.

Quantification of change response

The change response was quantified at the EEG electrode Pz across two experimental conditions (sitting and walking), as shown in Fig. 2a and Fig. 3a**.** The Pz electrode was identified based on peak detection in the ERP data, with the peak response following the change point observed at Pz. Time windows were predefined for the onset, change, and offset responses: [0, 300] ms for onset, [1050, 1350] ms for change, and [2000, 2300] ms for offset. Notably, the time window for the change response was shifted 50 ms later relative to onset and offset, reflecting the delayed peak latency of the change response compared to the other components.

To quantify the response at Pz for both the onset and change responses **(**Fig. 2c and Fig. 3c**),** the Response Magnitude (RM) was calculated. The RM is defined as the

Root Mean Square (RMS**)** of the normalized ERP within the predefined time window. Normalization was done by dividing each channel's ERP by its standard deviation over the entire trial. The RM calculation followed the formula:

$$\mathrm{RM}_i[t_1, t_2] = \sqrt{\frac{\sum_{t=t_1}^{t_2}[r_i(t)]^2}{n}}$$

where $r_i(t)$ represents the ERP of the ith channel at time t, n represents the number of samples within the time window from t_1 and t_2, and RM_i is the response magnitude of channel i. The RM was computed for each subject and condition (sitting and walking) within the predefined windows. The differential RM (ΔRM), defined as the difference in the response magnitude (RM), was calculated between the two experimental conditions, sitting and walking. Mathematically, it is expressed as:

$$\Delta RM = RMsit - RMwalk$$

Where RM_{sit} is the response magnitude for the sitting condition, and RM_{walk} is the response magnitude for the walking condition.

Psychological threshold

The ratio of change detection for each experimental condition was determined by dividing the number of trials in which the participant pressed the right arrow key (indicating perceived change) by the total number of trials in that condition. 47 participants were retained for standalone analyses of the change detection task. For comparisons between the change detection tasks across the two experimental conditions, all 47 participants were included.

Psychometric functions were fitted to the data using a cumulative Gaussian

model:

$$p(r) = \frac{1}{\sigma\sqrt{2\pi}} \int_{-\infty}^{r} e^{-\frac{(x-\mu)^2}{2\sigma^2}} dx$$

where $p(r)$ represents the ratio of change detection as a function of ICI r. μ is the Gaussian mean, and σ is the standard deviation (SD). The psychological threshold of change detection was defined as 0.6 of the Gaussian fit (Fig. 1d). This curve fitting procedure was achieved using the 'psignifit' software package (see http://bootstrap-software.org/psignifit/) for MATLAB.

Stride extraction from walking speed data

Stride phases were estimated from walking speed data using time-frequency analysis, specifically the wavelet transform (MATLAB function 'cwt'), to capture frequency variations over time and provide a detailed assessment of gait dynamics. The wavelet transform was applied to the speed data to generate the time-frequency response, from which the frequency with maximum spectral power at each time point was identified—typically within the 0.5–2 Hz range characteristic of walking gait (Fig. 4-5). Frequencies outside this range were deemed anomalous and replaced with the median of valid frequencies. The step phase was defined as the phase of the dominant frequency at each time point, with phase information unwrapped to eliminate discontinuities. Finally, phases were normalized to a stride cycle, encompassing two steps, with values ranging from 0 to 100%.

Analysis of Performance and Neural Response Relative to Stride. (Correct)

To assess the influence of stride cycle phase on auditory detection performance, the onset of each auditory target was assigned to its corresponding percentile (1–100%)

within the stride cycle, determined from gait phase extraction. For analysis, performance was averaged across 10 equal, non-overlapping bins (0–10%, 11–20%, ..., 91–100%) per cycle.

Auditory detection accuracy (hit rate) and reaction time were calculated for each stride-phase bin and each response type (onset, change, offset). Hit rate was defined as the proportion of correct responses; reaction time was measured as the interval between cue onset and participant response.

To determine the presence of significant oscillations in behavioral and neural measures across the stride cycle, a two-step procedure was used. First, at the group level, a series of sinusoidal (Fourier) models were fit to the binned data within a frequency range of 0.2 to 4 cycles per stride, in 0.1 cycle increments, using MATLAB's curve-fitting toolbox. Each model took the form:

$$f(t) = a0 + a1 \times \cos(\omega t) + b1 \times \sin(\omega t) = Acos(\omega t - \phi)$$

where ω is the periodicity (cycles per stride), t is time, $a1$ and $b1$ are the cosine and sine coefficients, and $a0$ is a constant, respectively. The resulting sinusoidal fit has amplitude A and phase □. A nonlinear least squares method was used to optimize the fit over 1000 iterations, and the goodness of fit (R^2) was calculated for each frequency. Next, to evaluate the statistical significance of the observed oscillations, we applied a non-parametric shuffling procedure. The data allocated to each percentile bin were shuffled independently for each subject (without replacement). After shuffling, the results were averaged across subjects, and the fitting procedure was repeated. This process was repeated 1000 times, generating a null distribution of R^2 values for each

frequency. A significant oscillation was defined when the observed R^2 value exceeded the critical value derived from the null distribution, accounting for multiple comparisons.

The above analyses were applied separately to the onset, change, and offset phases of auditory stimuli. Oscillations in hit rate and reaction time were assessed for each phase (Fig. 4c, d), revealing distinct patterns of performance modulation relative to the stride cycle.

For neural responses, the same Fourier analysis methodology was applied to model the oscillations in brain activity in response to auditory targets during the stride cycle for the onset, change, and offset phases. Additionally, the global quantification of the entire change response across the stride cycle for all three phases includes the relative response magnitude. (RM) was calculated, defined as the root mean square (RMS).

Statistics

To identify channels with significant change responses, the relative Response Magnitude (RM) of the change responses was computed for each channel and subject, as depicted in the topographic plots of RM (Fig. 2b and Fig. 3b). A two-tailed one-sample t-test was performed for each channel and subject, with p-values corrected within channels using the (Benjamini 2001)(false discovery rate [FDR] corrected). Channels with significant change responses were marked with black dots on the topographic plots.

For nonparametric tests, the Wilcoxon signed rank test (paired test) and the Mann-Whitney U test (unpaired test) was used. The effect size was computed using the r-value. The r-value was measured and calculated by using the formula:

$$r = Z/\sqrt{N}$$

Furthermore, to compute the effect size for each channel, Cohen's d was calculated using the formula:

$$d = \frac{\overline{X} - \overline{Y}}{\sqrt{\frac{1}{N-1}\sum_{i=1}^{N}\left(X_i - Y_i - \left(\overline{X} - \overline{Y}\right)\right)^2}}$$

where d represents Cohen's d. X and Y are the paired samples with a total number of N (all Y as zero for a one-sample t-test). X_i and Y_i are the ith elements from the paired samples. $\overline{X}$ and $\overline{Y}$ are mean values of the samples.

This method was employed to measure the change response magnitude for each subject and channel in both sitting and walking conditions. The RM was calculated for each subject and condition (sitting and walking) within the predefined time windows for the onset, change, and offset responses

To identify channels with a significant difference in response between correct and incorrect trials in the change detection behavioural task across two experimental conditions, a two-tailed Wilcoxon signed rank test was also performed on the average response relative to the change point, centered around the estimated peak time for each channel.

To test whether there was a clear tuning of RM in the two conditions, a one-way ANOVA was performed among the five contrasted groups ($Reg_{4\text{-}4}$, $Reg_{4\text{-}4.01}$, $Reg_{4\text{-}4.02}$,

$Reg_{4\text{-}4.03}$, and $Reg_{4\text{-}4.06}$). The effect size of the one-way ANOVA was measured using Eta-squared (η^2):

$$\eta^2 = \frac{SS_{between}}{SS_{total}}$$

where $SS_{between}$ is the sum of squared variation due to the factor (between groups). SS_{total} is the total sum of squared variation in the data.

Bayesian statistical analyses were conducted to quantify evidence for the null hypothesis across different types of comparisons. For pairwise comparisons, we used Bayesian paired-sample t-tests with a Jeffreys-Zellner-Siow (JZS) prior, as described by (Rouder, Speckman et al. 2009). For group comparisons involving more than two levels, we employed Bayesian one-way ANOVA, using default Cauchy priors on effect sizes. To assess associations between continuous variables, we conducted Bayesian correlation analyses based on a Jeffreys prior for Pearson's correlation coefficient. All Bayes factors (BF_{10}) were computed using the BayesFactor toolbox for MATLAB. A BF_{10} greater than 1 indicates evidence in favour of the alternative hypothesis, whereas a BF_{10} less than 1 indicates evidence in favour of the null.

Figure legends

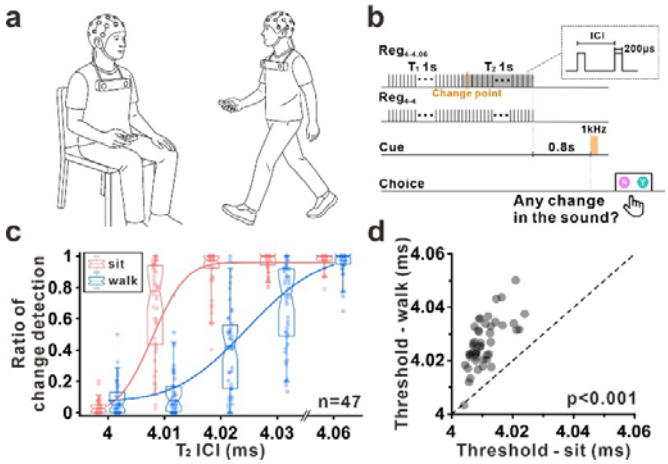

Figure 1. Experimental setup and change detection thresholds during sitting and walking conditions. (a) Schematic diagram of the experimental setup, showing the participant in either seated (left) or walking (right) positions, equipped with wireless EEG caps and a button for change detection tasks. The experimental setup is designed to record neural activity in participants across different postural conditions (sitting vs walking), focusing on auditory change detection. **(b)** Layout of the auditory stimulation setup (transitional click train). Two click trains, each comprising 0.2-ms monopolar pulses with different inter-click intervals (ICIs), were linked seamlessly to create a transitional click train. For example, one at 4 ms—train 1 (T_1) and the other at 4.06 ms—train 2 (T_2) were referred to as $Reg_{4\text{-}4.06}$. Five stimuli ($Reg_{4\text{-}4}$, $Reg_{4\text{-}4.01}$, $Reg_{4\text{-}4.02}$, $Reg_{4\text{-}4.03}$, and $Reg_{4\text{-}4.06}$) were presented in random order. After each click train, a 1 kHz cue (100-ms duration) was presented 800 ms after the end of the click train. Participants were instructed to indicate whether a change occurred across the transitional click train via button presses. Wireless button presses were valid within 2 seconds after the cue onset. (c) Ratio of change detection as a function of the T_2 ICIs during sitting (red) and walking (blue) conditions (n = 47; median: central line;

25th-75th percentiles: box edges; 5th–95th percentiles: whiskers). Transparent dots represent individual participants. (d) Scatter plot comparing change detection thresholds between sitting and walking conditions (n = 47), with $p < 0.001$ for a two-tailed paired t-test.

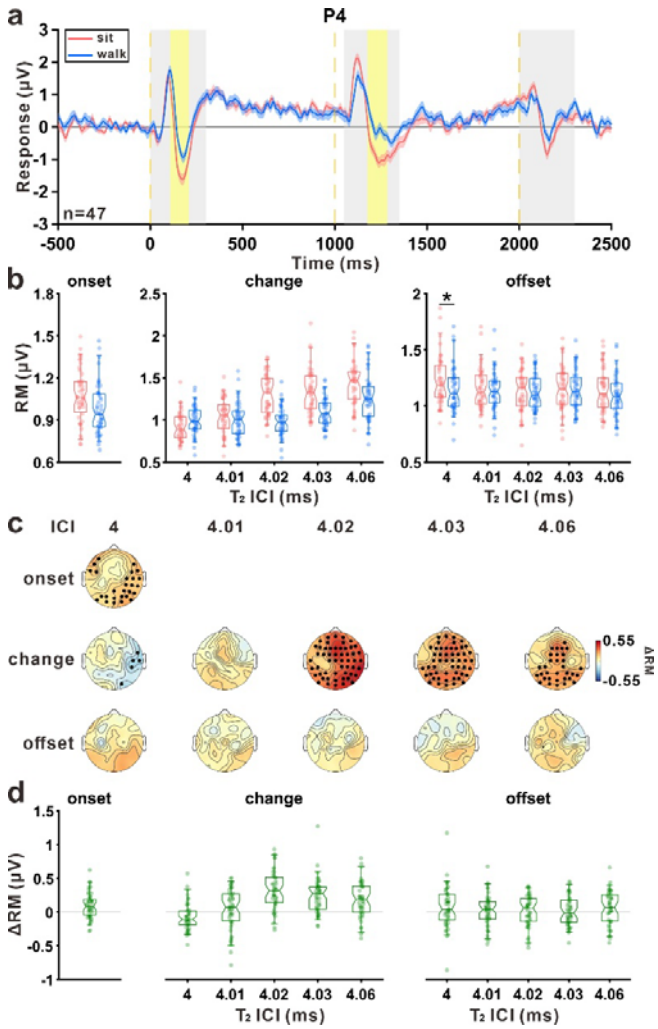

Figure 2. Walking selectively modulates auditory onset and change responses.

(a) Grand-averaged event-related potentials (ERPs) at the P4 electrode during sitting (red) and walking (blue) conditions (n = 47). Shaded regions (gray) indicate the analysis windows for onset, change, and offset responses, respectively, while yellow

highlights indicate significant differences ($p < 0.05$, permutation test). Vertical orange dashed lines denote the onset (0 ms), change (1000 ms), and offset (2000 ms) of the transitional click train. **(b)** Response magnitude (RM; root mean square amplitude) for onset, change, and offset responses across the five T□ ICI conditions for sitting (red) and walking (blue). Each dot represents an individual participant. Notched boxplots showing the median (line), interquartile range (box: 25th–75th percentiles), and data spread (whiskers: 5th–95th percentiles). Notches indicate the 95% confidence interval of the median. Significant differences between sitting and walking conditions are indicated by asterisks (*$p < 0.05$, two-tailed paired t-test). **(c)** Topographical maps showing the difference in response magnitude (sit minus walk) for onset, change, and offset responses across T□ ICI conditions. Dots indicate electrodes with significant differences ($p < 0.05$, FDR-corrected, two-tailed paired t-test). **(d)** Distribution of ΔRM (sit – walk) for onset, change, and offset responses across T□ ICI conditions. Each dot represents an individual participant.

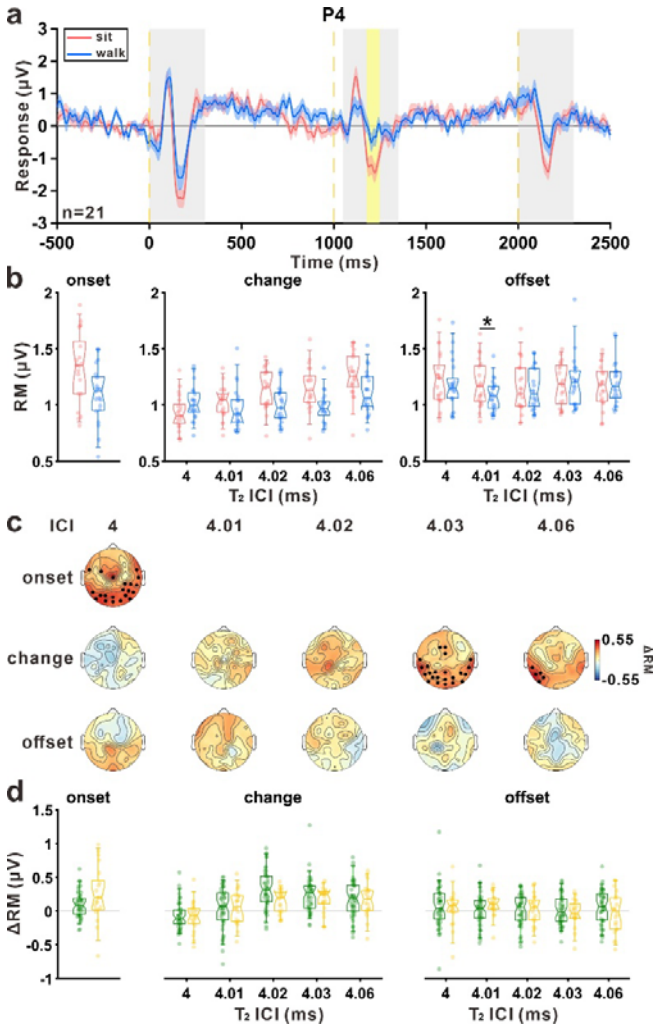

Figure 3. Walking-induced modulation of auditory responses during passive listening. (a) Grand-averaged event-related potentials (ERPs) at the P4 electrode during sitting (red) and walking (blue) conditions in the passive listening experiment (n = 21). Shaded regions (gray) indicate the analysis windows for onset, change, and offset responses; yellow highlights indicate significant differences ($p < 0.05$, permutation test). Vertical orange dashed lines mark the onset (0 ms), change (1000 ms), and offset (2000 ms) of the transitional click train. **(b)** Response magnitude (RM; root mean square amplitude) for onset, change, and offset responses across the five T□ ICI conditions for sitting (red) and walking (blue). Each dot represents an

individual participant. Notched boxplots showing the median (line), interquartile range (box: 25th–75th percentiles), and data spread (whiskers: 5th–95th percentiles). Significant differences between sitting and walking conditions are marked with asterisks (*$p < 0.05$, two-tailed paired t-test). **(c)** Topographical maps showing the difference in response magnitude (sit minus walk) for onset, change, and offset responses across T□ ICI conditions. Dots indicate electrodes with significant differences ($p < 0.05$, FDR-corrected, two-tailed paired t-test). **(d)** Distribution of ΔRM (sit – walk) for onset, change, and offset responses across T□ ICI conditions, shown separately for behavioral (green) and non-behavioral (yellow) conditions. Each dot represents an individual participant. Asterisks denote significant differences between behavioral and non-behavioral conditions (*$p < 0.05$, two-tailed Mann-Whitney U test).

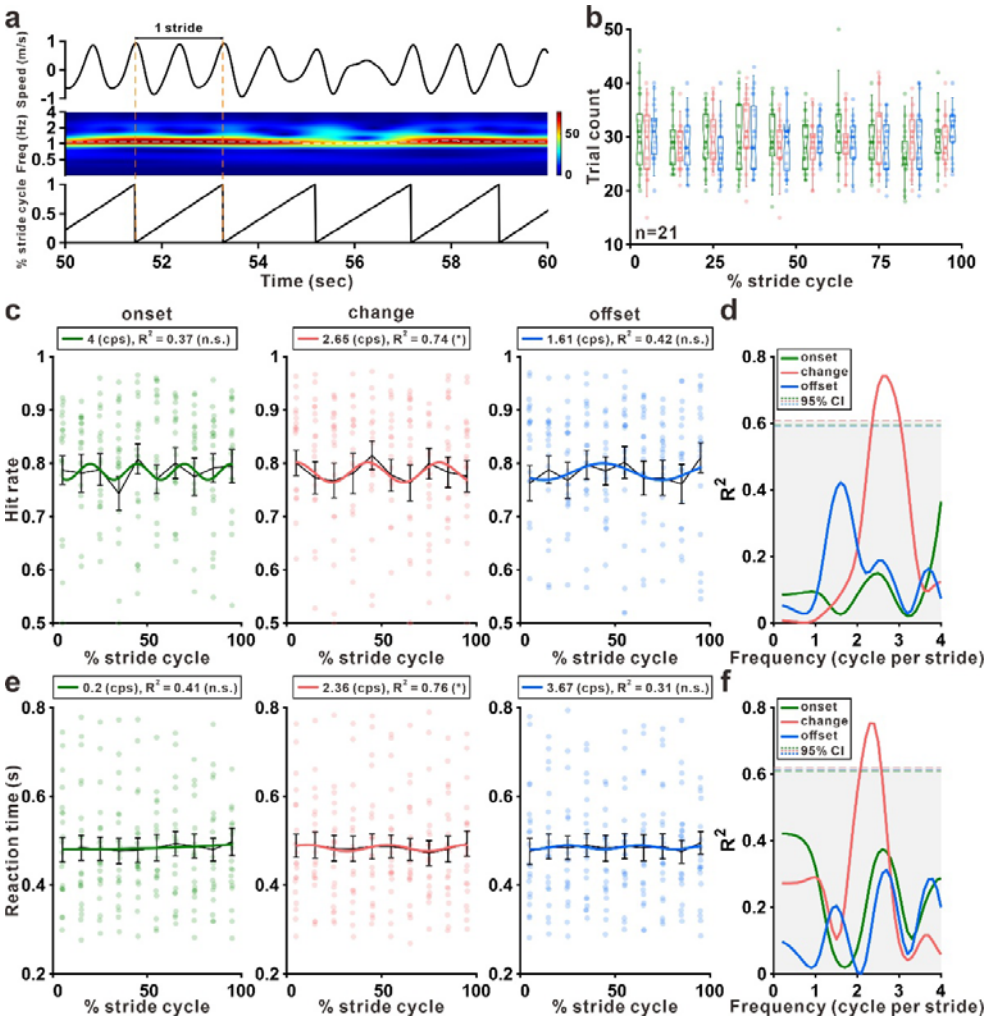

Figure 4. Performance oscillates within the stride cycle. (a) Example of stride cycle identification from a single participant. The top panel shows walking speed (m/s) as a function of time (s); the middle panel displays the time-frequency response (continuous wavelet transform) with spectral power indicated by color scale; the bottom panel aligns extracted stride cycles, with vertical dashed lines marking completed strides. Each stride (comprising two steps) was resampled to a normalized 1–100% range to enable pooling across individuals. **(b)** Binned scatter plot of trial counts for each stride-cycle bin (10 bins of 10% each), pooled across all 21 subjects with hit rate below 1. Notched boxplots showing the median (line), interquartile range

(box: 25th–75th percentiles), and data spread (whiskers: 5th–95th percentiles). The distribution of trials for Reg4-4.06 was approximately uniform across the stride cycle. **(c, e)** Group-level data (n = 21) depicting detection accuracy (hit rate, **c**) and reaction time (**e**) as a function of stride-cycle phase for three auditory response types: onset (green), change (red), and offset (blue). Data are shown for 10% increments; each dot represents an individual participant. Solid curves show the best-fitting order-Fourier model for each phase. **(d, f)** Permutation testing of the best-fitting Fourier models for hit rate (**d**) and reaction time (**f**). Observed data (from c and e) were fit with single-component Fourier models across frequencies from 0.2 to 4 cycles per stride (in 0.1 cps steps), and goodness-of-fit (R^2) was calculated to assess variation in auditory performance as a function of stride-cycle frequency. Prominent peaks reveal the best fits for the change phase (red) at ~2.7 cps (hit rate) and ~2.4 cps (reaction time), both far exceeding the 95% permutation confidence interval (dotted lines and grey shading). Onset (green) and offset (blue) phases peaked at ~4 and ~1.6 cps for hit rate, and at ~0.2 and ~3.7 cps for reaction time, respectively. The likelihood of target presentation (grey line) did not show above-chance fluctuations coincident with these peaks.

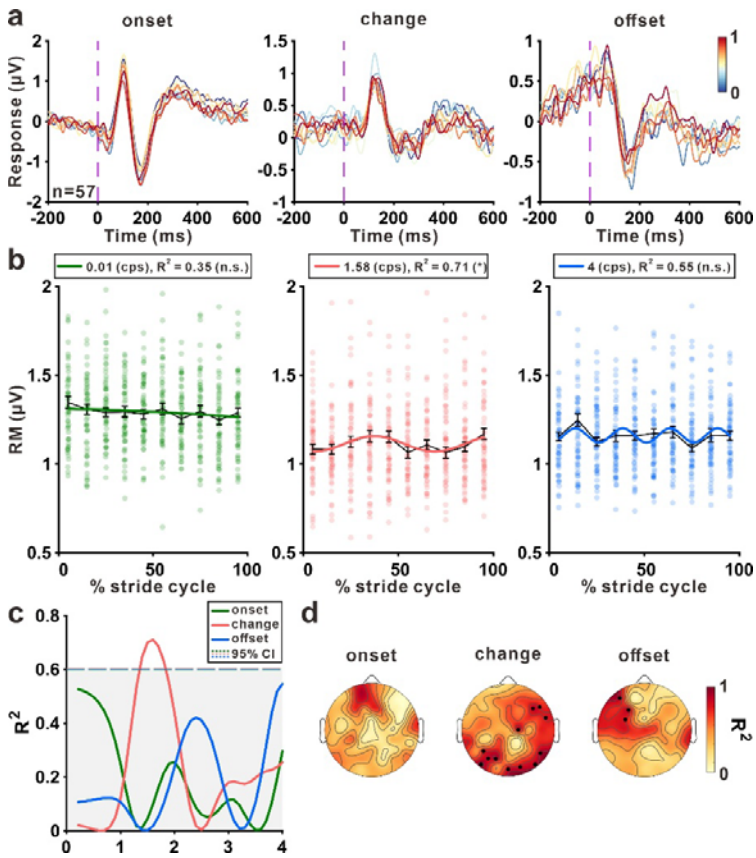

Figure 5. EEG results within the stride cycle. (a) Grand-averaged responses for three auditory phases: onset (left), change (middle), and offset (right) across 57 participants. The color bar represents the stride cycle bins. **(b)** Group-level data (n = 57) showing response magnitude (RM) as a function of stride-cycle phase for onset (green), change (red), and offset (blue) responses. Data are binned in 10% increments; black lines represent mean ± S.E.M., dots indicate individual values. **(c)** Permutation testing of the best-fitting Fourier models. Observed data from (b) were fitted using the same Fourier modeling procedure as in Figures 4d and 4f. The prominent peak for the change phase (red) at approximately 1.6 cycles per stride indicates significant rhythmic modulation, while the onset and offset phases showed no significant modulation. The shaded region represents the 95% permutation confidence interval,

calculated using the maximum test statistic across all frequencies per permutation (dotted lines and grey shading) for each phase. **(d)** Topographic maps showing the spatial distribution (R^2) of stride-phase modulation in neural responses for onset, change, and offset phases. Dots indicate electrodes with significant modulation ($p < 0.05$, two-tailed paired t-test, FDR-corrected). R^2 values represent the goodness of fit between neural response and stride cycle for each phase.

References:

1. Asilador, A. and D. A. Llano (2020). "Top-Down Inference in the Auditory System: Potential Roles for Corticofugal Projections." Front Neural Circuits **14**: 615259.
2. Auksztulewicz, R., O. B. Ödül, S. Helbling, A. Böke, D. Cappotto, D. Luo, J. Schnupp and L. Melloni (2025). ""What" and "When" Predictions Jointly Modulate Speech Processing." J Neurosci **45**(20).
3. Benjamini, Y. Y., D. (2001). ""The control of the false discovery rate in multiple testing under dependency." " Annals of Statistics **29:** : 1165-1188.
4. Davidson, M. J., F. A. Verstraten and D. Alais (2024). "Walking modulates visual detection performance according to stride cycle phase." Nature communications **15**(1): 2027.
5. Delval, A., M. Bayot, L. Defebvre and K. Dujardin (2020). "Cortical Oscillations during Gait: Wouldn't Walking be so Automatic?" Brain Sci **10**(2).
6. Di Stefano, N. and C. Spence (2025). "Perceiving temporal structure within and between the senses: A multisensory/crossmodal perspective." Atten Percept

Psychophys **87**(5): 1811-1838.

7. Dionne-Dostie, E., N. Paquette, M. Lassonde and A. Gallagher (2015). "Multisensory integration and child neurodevelopment." Brain Sci **5**(1): 32-57.
8. Donato, R., A. Contillo, G. Campana, M. Roccato, Ó. F. Gonçalves and A. Pavan (2024). "Visual Perceptual Learning of Form–Motion Integration: Exploring the Involved Mechanisms with Transfer Effects and the Equivalent Noise Approach." Brain Sciences **14**(10): 997.
9. Du, X., H. Xu, P. Song, Y. Zhai, H. Ye, X. Bao, Q. Huang, H. Tanigawa, Z. Tu, P. Chen, X. Zhao, J. P. Rauschecker and X. Yu (2025). "The multifaceted role of the inferior colliculus in sensory prediction, reward processing, and decision-making." Elife **13**.
10. Gong, Y., P. Song, X. Du, Y. Zhai, H. Xu, H. Ye, X. Bao, Q. Huang, Z. Tu, P. Chen, X. Zhao, D. Pérez-González, M. S. Malmierca and X. Yu (2024). "Neural correlates of novelty detection in the primary auditory cortex of behaving monkeys." Cell Rep **43**(3): 113864.
11. Hentschke, H., F. Haiss and C. Schwarz (2006). "Central signals rapidly switch tactile processing in rat barrel cortex during whisker movements." Cereb Cortex **16**(8): 1142-1156.
12. Kraus, N., E. Skoe, A. Parbery-Clark and R. Ashley (2009). "Experience-induced malleability in neural encoding of pitch, timbre, and timing." Ann N Y Acad Sci **1169**: 543-557.
13. Li, S.-C., E. Muschter, J. Limanowski and A. Hatzipanayioti (2021). "Human perception and neurocognitive development across the lifespan." Tactile internet:

199-221.

14. Lickliter, R. (2011). "The integrated development of sensory organization." Clin Perinatol **38**(4): 591-603.

15. Liebherr, M., A. W. Corcoran, P. M. Alday, S. Coussens, V. Bellan, C. A. Howlett, M. A. Immink, M. Kohler, M. Schlesewsky and I. Bornkessel-Schlesewsky (2021). "EEG and behavioral correlates of attentional processing while walking and navigating naturalistic environments." Sci Rep **11**(1): 22325.

16. McPhee, A. M., T. C. K. Cheung and M. A. Schmuckler (2022). "Dual-task interference as a function of varying motor and cognitive demands." Front Psychol **13**: 952245.

17. Morillon, B. and S. Baillet (2017). "Motor origin of temporal predictions in auditory attention." Proc Natl Acad Sci U S A **114**(42): E8913-e8921.

18. Morillon, B., C. E. Schroeder and V. Wyart (2014). "Motor contributions to the temporal precision of auditory attention." Nat Commun **5**: 5255.

19. Nabé, M., J.-L. Schwartz and J. Diard (2021). "Cosmo-onset: A neurally-inspired computational model of spoken word recognition, combining top-down prediction and bottom-up detection of syllabic onsets." Frontiers in Systems Neuroscience **15**: 653975.

20. Noboa, M. L., C. Kertész and F. Honbolygó (2025). "Neural entrainment to the beat and working memory predict sensorimotor synchronization skills." Sci Rep **15**(1): 10466.

21. Oostenveld, R., P. Fries, E. Maris and J. M. Schoffelen (2011). "FieldTrip: Open source software for advanced analysis of MEG, EEG, and invasive

electrophysiological data." Comput Intell Neurosci **2011**: 156869.

22. Parker, P. R., M. A. Brown, M. C. Smear and C. M. Niell (2020). "Movement-related signals in sensory areas: roles in natural behavior." Trends in neurosciences **43**(8): 581-595.
23. Parker, P. R. L., M. A. Brown, M. C. Smear and C. M. Niell (2020). "Movement-Related Signals in Sensory Areas: Roles in Natural Behavior." Trends Neurosci **43**(8): 581-595.
24. Pranjić, M., T. Braun Janzen, N. Vukšić and M. Thaut (2024). "From Sound to Movement: Mapping the Neural Mechanisms of Auditory-Motor Entrainment and Synchronization." Brain Sci **14**(11).
25. Proksch, S., D. C. Comstock, B. Médé, A. Pabst and R. Balasubramaniam (2020). "Motor and Predictive Processes in Auditory Beat and Rhythm Perception." Front Hum Neurosci **14**: 578546.
26. Rauschecker, J. P. (1998). "Cortical processing of complex sounds." Current opinion in neurobiology **8**(4): 516-521.
27. Riedel, N., M. Herzog, T. Stein and B. Deml (2024). "Cognitive-motor interference during walking with modified leg mechanics: a dual-task walking study." Front Psychol **15**: 1375029.
28. Rouder, J. N., P. L. Speckman, D. Sun, R. D. Morey and G. Iverson (2009). "Bayesian t tests for accepting and rejecting the null hypothesis." Psychon Bull Rev **16**(2): 225-237.
29. Rubega, M., R. Di Marco, M. Zampini, E. Formaggio, E. Menegatti, P. Bonato, S.

Masiero and A. Del Felice (2021). "Muscular and cortical activation during dynamic and static balance in the elderly: A scoping review." Aging Brain **1**: 100013.

30. Salvucci, D. D. and N. A. Taatgen (2008). "Threaded cognition: an integrated theory of concurrent multitasking." Psychol Rev **115**(1): 101-130.
31. Senkowski, D. and A. K. Engel (2024). "Multi-timescale neural dynamics for multisensory integration." Nat Rev Neurosci **25**(9): 625-642.
32. Song, P., H. Xu, H. Ye, X. Du, Y. Zhai, X. Bao, Q. Huang, I. Mehmood, H. Tanigawa, W. Niu, Z. Tu, P. Chen, T. Zhang, X. Zhao and X. Yu (2025). "Temporal merging into pitch with click train in the macaque auditory cortex." Natl Sci Rev **12**(6): nwaf026.
33. Song, P., H. Xu, H. Ye, X. Du, Y. Zhai, X. Bao, I. Mehmood, H. Tanigawa, W. Niu and Z. Tu (2024). "A new function of offset response in the primate auditory cortex: marker of temporal integration." Communications Biology **7**(1): 1350.
34. Starke, J., F. Ball, H. J. Heinze and T. Noesselt (2020). "The spatio-temporal profile of multisensory integration." Eur J Neurosci **51**(5): 1210-1223.
35. Stuart, S., R. Vitorio, R. Morris, D. N. Martini, P. C. Fino and M. Mancini (2018). "Cortical activity during walking and balance tasks in older adults and in people with Parkinson's disease: A structured review." Maturitas **113**: 53-72.
36. Tallal, P., S. Miller and R. H. Fitch (1993). "Neurobiological basis of speech: a case for the preeminence of temporal processing." Ann N Y Acad Sci **682**: 27-47.
37. Tomassini, A., D. Spinelli, M. Jacono, G. Sandini and M. C. Morrone (2015). "Rhythmic oscillations of visual contrast sensitivity synchronized with action." Journal of Neuroscience **35**(18): 7019-7029.

38. Wachsmann, F. D., K. Fiehler and D. Voudouris (2025). "Temporal modulation of tactile perception during balance control." Sci Rep **15**(1): 17380.

39. Xu, H., Q. Huang, P. Song, Y. Chen, Q. Li, Y. Zhai, X. Du, H. Ye, X. Bao, I. Mehmood, H. Tanigawa, W. Niu, Z. Tu, P. Chen, T. Zhang, L. Zhang, X. Zhao, L. Zhang, W. Wen, L. Cao and X. Yu (2025). "EEG neural indicator of temporal integration in the human auditory brain with clinical implications." Commun Biol **8**(1): 1109.

40. Zagha, E., A. E. Casale, R. N. Sachdev, M. J. McGinley and D. A. McCormick (2013). "Motor cortex feedback influences sensory processing by modulating network state." Neuron **79**(3): 567-578.

41. Zalta, A., S. Petkoski and B. Morillon (2020). "Natural rhythms of periodic temporal attention." Nat Commun **11**(1): 1051.

42. Zheng, Y., J. Zhang, Y. Yang and M. Xu (2025). "Neural representation of sensorimotor features in language-motor areas during auditory and visual perception." Communications Biology **8**(1): 41.